Isotopic and microcanonical temperatures in nuclear multifragmentation

J. P. Bondorf,[1] A. S. Botvina,[2,3] and I. N. Mishustin[1,4]
[1]*Niels Bohr Institute, DK-2100 Copenhagen Ø, Denmark*
[2]*Dipartimento di Fisica and INFN, 40126 Bologna, Italy*
[3]*Institute for Nuclear Research, Russian Academy of Science, 117312 Moscow, Russia*
[4]*Kurchatov Institute, Russian Scientific Center, 123182 Moscow, Russia*
(Received 7 April 1997)

A systematic comparison of different isotopic temperatures with the thermodynamical temperature of a multifragment system is made on the basis of the statistical multifragmentation model. It is demonstrated that isotopic temperatures are strongly affected by the secondary decays of hot primary fragments and the population of particle-stable excited states in final fragments. The He-Li temperatures, measured recently by the ALADIN group, are reproduced fairly well both as a function of excitation energy and bound charge. Our analysis confirms the anomaly in the nuclear caloric curve. [S0556-2813(98)50507-9]

PACS number(s): 25.70.Pq, 21.65.+f, 24.10.Pa, 24.60.Ky

Presently nuclear multifragmentation in heavy-ion reactions is intensively studied, both theoretically and experimentally. One of the main goals is to investigate properties of nuclear matter away from the ground state. A most interesting question here is how multifragmentation is related to a liquid-gas phase transition in a finite nuclear system. To answer this question one needs observables which bring information about the thermodynamical state of the system, in particular, its excitation energy and temperature. Then a phase transition should manifest itself by an anomaly in the caloric curve, i.e., temperature as a function of excitation energy. According to the statistical model prediction [1], the nuclear caloric curve behaves like in an ordinary liquid-gas phase transition: initially the temperature increases, at excitation energies between 3 and 10 MeV/nucleon it stays almost constant at about 5–6 MeV, and then grows again. The first regime corresponds to the compound nucleus (liquid phase), the second one, to the multifragment mixture (coexistence phase), and the third one, to an assembly of nucleons and lightest clusters (gaseous phase).

The first measurements of the nuclear caloric curve have been made only recently by the ALADIN group [2]. They indeed revealed an anomalous behavior of the nuclear caloric curve similar to that predicted by the statistical model [1]. In the experiment the so-called isotopic temperature $T_{\rm isot}$ was extracted from the double ratio of helium and lithium isotope yields. At present nuclear temperature measurements are in fast progress. Several groups have reported results on nuclear caloric curves for different reactions and with different isotope thermometers [3–6]. Therefore, it is very important now to understand how these isotopic temperatures are related to the thermodynamical temperatures of excited nuclear systems at the stage of their breakup.

According to the method suggested by Albergo *et al.* [7], the isotopic temperature is expressed through the double ratio of isotope yields as

$$T_{\rm isot}=\frac{B}{\ln(a\cdot R)}. \tag{1}$$

Here $R=(Y_1/Y_2)/(Y_3/Y_4)$, $B=(B_1-B_2)-(B_3-B_4)$. Y_i and B_i are the ith isotope yield and binding energy, a is a constant determined by spin degeneracy factors and masses of the isotopes. The indexes $i=1$, 2, 3, and 4 refer to the isotopes with masses and charges (A,Z), $(A+1,Z)$, (A',Z') and $(A'+1,Z')$, respectively.

It is clear that this expression corresponds to the grand canonical approximation assuming thermal and chemical equilibrium. Moreover, it is assumed that all fragments are produced simultaneously at the same T and only in their ground states. These assumptions are too crude for finite and highly excited nuclear systems under consideration. A more realistic approach should include at least two important modifications: first, the microcanonical treatment of the break-up channels, i.e., taking into account exact conservation laws for baryon number, charge, and energy, and second, the feeding of isotope yields from the de-excitation of hot primary fragments after the breakup. The importance of secondary decays was demonstrated earlier by several authors (see, e.g., Refs. [8–10]). Statistical models of multifragmentation (see reviews [11,12]) provide a natural framework for introducing these modifications. These models are very successful in describing many observed characteristics of nuclear multifragmentation (see examples in Refs. [13,14]).

The calculations below are made within the standard version of the statistical multifragmentation model (SMM) which was used for the first calculation of the nuclear caloric curve [1]. Here we outline only some general features of the model (see details in Ref. [12]). It is assumed that at the breakup time the system consists of primary hot fragments and nucleons in thermal equilibrium. Each breakup channel f is specified by the multiplicities of different species N_{AZ}, which are constrained by the total baryon number A_0 and charge Z_0 of the system. The probabilities of different breakup channels are calculated in an approximate microcanonical way according to their statistical weights, $W_f \propto \exp[S_f(E^*,V,A_0,Z_0)]$, where S_f is the entropy of a channel f at excitation energy E^* and breakup volume V.

Translational degrees of freedom of individual fragments are described by the Boltzmann statistics while the internal excitations of fragments with $A>4$ are calculated within the

liquid-drop model with Fermi-gas level density. An ensemble of microscopic states corresponding to the breakup channel f is characterized by a temperature T_f which is determined from the energy balance equation

$$\frac{3}{2}T(m-1)+\sum_{(A,Z)} E_{AZ}(T)N_{AZ}+E_f^C(V)-Q_f=E^*. \quad (2)$$

Here $m=\Sigma N_{AZ}$ is the total fragment multiplicity, the first term comes from the translational motion, the second term includes internal excitation energies of individual fragments, and the third term is the Coulomb interaction energy, Q_f is the Q value of the channel f. The excitation energy E^* is measured with respect to the ground state of the compound nucleus (A_0,Z_0). In our semimicrocanonical treatment E^* is fixed for all fragmentation channels while the temperature T_f fluctuates from channel to channel.

The total breakup volume is parametrized as $V=(1+\kappa)V_0$, where V_0 is the compound nucleus volume at normal density and the model parameter κ is the same for all channels. The choice of κ is motivated by the requirements (a) to avoid overlaps between the fragments and (b) to provide a sufficient reduction of the Coulomb barrier, as seen in the kinetic energy spectra. The entropy associated with the translational motion of fragments is determined by the ''free'' volume, V_f, which incorporates the excluded volume effects. In general V_f depends on the breakup channel and therefore cannot be fixed to a constant κV_0, as often assumed. In the SMM we parametrize $V_f(m)$ in such a way that it grows almost linearly with the primary fragment multiplicity m or, equivalently, with the excitation energy $\varepsilon^*=E^*/A_0$ of the system [12]. According to this parametrization, $V_f(m)$ vanishes for the compound nucleus $(m=1)$ and increases to about $2V_0$ at $\varepsilon^*\approx$ 10 MeV/nucleon.

At given inputs A_0, Z_0, and ε^* the individual multifragment configurations are generated by the Monte Carlo method. After the breakup hot primary fragments loose their excitation. The most important deexcitation mechanisms included in the SMM [12] are the simultaneous Fermi breakup of lighter fragments $(A\leqslant 16)$ and the evaporation from heavier fragments, including the compoundlike residues. In this respect SMM essentially differs from the QSM type models [10] where the compoundlike channels are completely ignored (see discussion in Ref. [15]).

Now we turn to numerical simulations of the multifragmentation on the basis of SMM. First of all we present results for a well defined source, i.e., an excited ^{197}Au nucleus. The caloric curve is calculated by first solving Eq. (2) for each particular channel and then averaging T_f over a large number of breakup channels. In Fig. 1 (top) different curves correspond to different choices of volume parameters. If the standard parametrization $V_f(m)$ is used, the caloric curve is quite flat in the ε^* region between 3 and 10 MeV/nucleon. This is a signature of a large heat capacity in the transition region. Even a backbending is possible if the total volume V is not very large, say, only $3V_0$ $(\kappa=2)$. In contrast, if the free volume would be fixed to $V_f=\kappa V_0$ for all channels, the temperature would increase gradually with ε^*. Nevertheless, as seen in Fig. 1, some flattening in the caloric curve is predicted also in this case. The reason for the different behavior is clear: at $\varepsilon^*<10$ MeV/nucleon the multiplicity-dependent

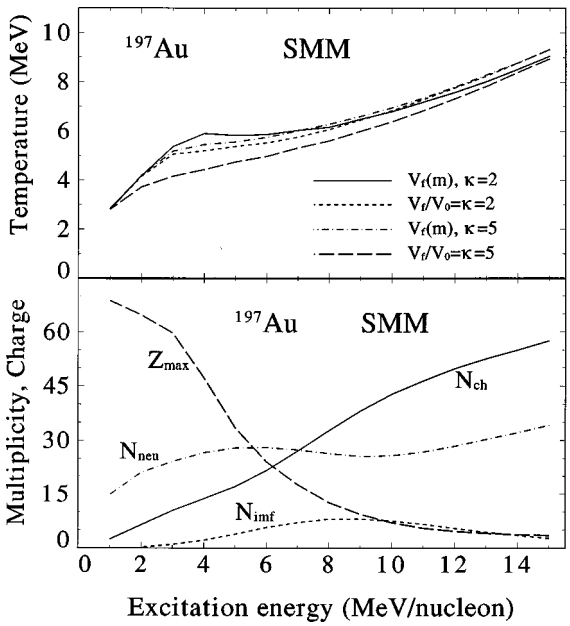

FIG. 1. Top: Caloric curves as predicted by the SMM simulations for an excited ^{197}Au nucleus. Results are shown for four different choices of volume parameters characterizing the breakup configuration (see the text). Bottom: Some observable characteristics as functions of excitation energy in multifragmentation of ^{197}Au nucleus after deexcitation of primary fragments. $Z_{\max}$ is the maximum fragment charge; $N_{\rm imf}$ is the multiplicity of intermediate mass fragments $(3\leqslant Z\leqslant 20)$; $N_{\rm ch}$ and $N_{\rm neu}$ are the total numbers of charged particles and free neutrons.

free volume $V_f(m)$ is smaller than κV_0 that leads to a higher temperature of the system. In the following calculations we use $\kappa=2$ and the standard SMM parametrization of $V_f(m)$, which gives a plateau in the caloric curve. As we will see below such behavior is favored by the data.

The characteristics of the system change drastically when ε^* increases from 3 to 10 MeV/nucleon. In the lower part of Fig. 1 we display several observables calculated after the completion of all secondary decays. A heavy residue, usual for the evaporationlike processes, practically disappears. This is signaled by the maximum fragment charge $Z_{\max}$, which drops rapidly from 60 to about 6 in this region. At the same time, the number of intermediate mass fragments (IMFs: $3\leqslant Z\leqslant 20$) first increases and then goes through the maximum, $N_{\rm imf}\approx$ 8, in the end of this region. The multiplicity of all charged particles $N_{\rm ch}$ grows with ε^* almost linearly. It is interesting to note that in the transition region the number of free neutrons $N_{\rm neu}$ is almost constant and close to the neutron excess in the initial ^{197}Au nucleus. This happens because the system breaks up predominantly into fragments with $N\approx Z$ (see also [15]). By comparing upper and lower parts of Fig. 1 one can conclude that the neutron multiplicity is nearly proportional to the temperature of the system but not to the excitation energy.

We have also calculated final isotope yields in the disintegration of an ^{197}Au nucleus. Several isotopic temperatures were obtained by applying formula (1) to different isotope pairs. Results are shown in Fig. 2 together with the microcanonical temperature $T_{\rm micr}$. One can see that the plateau is almost washed out and all isotopic temperatures increase

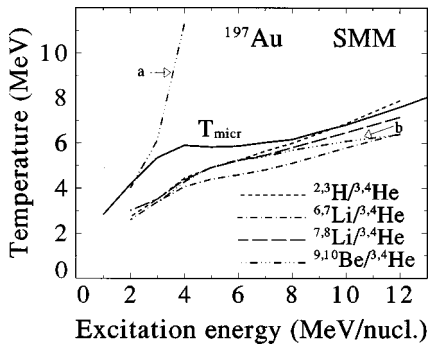

FIG. 2. Isotopic temperatures for four isotope pairs (indicated in the figure) versus excitation energy calculated for ^{197}Au by applying formula (1) to final isotope yields. The microcanonical temperature of the decaying nucleus is shown by the solid line.

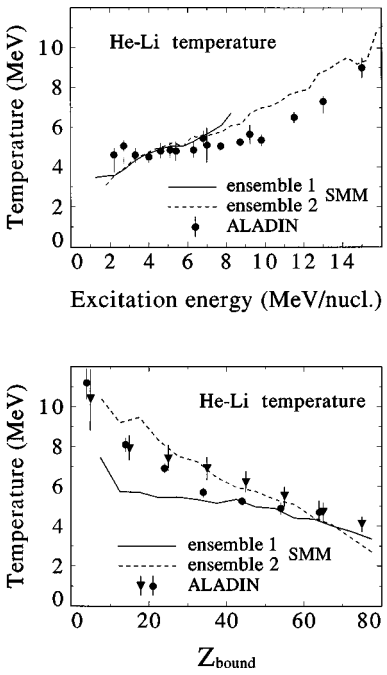

FIG. 3. He-Li temperatures (scaled by factor 1.2) versus excitation energy ε^* (top) and bound charge Z_{bound} (bottom) for projectile spectators produced in Au+Au collisions at 0.6*A* and 1.0*A* GeV. Symbols represent the ALADIN data for 0.6*A* GeV [2,16] (dots) and 1.0*A* GeV [16] (triangles). The SMM calculations are made for two ensembles of thermalized sources: 1 from Ref. [13] and 2 from Ref. [2].

gradually with ε^*. This behavior can be explained by the deexcitation of hot primary fragments leading to their cooling and side feeding of isotope yields. Since the energy conservation is controlled at all stages of the calculations, the SMM leads naturally to the cooling of emitters in endothermic processes responsible for the fragment deexcitation. In the case of sequential evaporation the first fragments are emitted from a source characterized by the emission temperature T_{micr}. But the next generation of fragments comes from a cooler residue leading to a lower apparent temperature [5]. This cooling mechanism can partly explain the difference between the isotopic temperatures and T_{micr} at lower excitation energies ($\varepsilon^*=1-6$ MeV/nucleon), when heavy residues ($Z_{max}>20$) survive in the breakup. At $\epsilon^*\geqslant 3$ MeV/nucleon another deexcitation mechanism becomes increasingly important, i.e., the one-step Fermi breakup where only particle-stable decay products are allowed. It is mainly responsible for the production of light isotopes, in particular He and Li, through the deep disintegration of heavier fragments ($A\sim 15$). Since the available energy (per nucleon) is considerably lower in this process than in the primary breakup, the apparent isotopic temperatures are also lower. Finally, at high excitation energies, $\epsilon^*\geqslant 10$ Mev/nucleon, when predominantly light fragments are formed, the reduction of the available energy for secondary breakup becomes less important and isotopic temperatures, in average, approach T_{micr}.

From Fig. 2 one can also see that the temperature measurements can be significantly obscured by the irregularities in the excited states of light fragments. In our standard calculations the final isotope yields include the fragments in particle-stable ground and excited states decaying by the γ emission. For the considered isotopes they are 3.56 MeV for ^{6}Li, 0.48 MeV for ^{7}Li, 0.43 MeV for ^{8}Li, 3.37, 5.96, 6.18, and 6.26 MeV for ^{10}Be. No such excited states are seen in ^{3,4}He and ^{9}Be and therefore only ground states are included for these nuclei. One can see that the deviations from the true temperature are especially large (curve *a*) in the case when one of the isotopes has many and the other, only a few or no excited states, e.g., in the ^{10}Be-^{9}Be pair. If the excited states in ^{10}Be are artificially switched off, the corresponding isotopic temperature (curve *b*) changes drastically and follows the common trend. To suppress the fluctuations associated with the nuclear structure effects one can use an ensemble of isotope thermometers as suggested in Ref. [3]. Another possibility is to use isotope pairs with only a few low-lying states which almost compensate each other, e.g., ^{7}Li-^{8}Li. In this respect it is preferable to use thermometers with isotopes no heavier than lithium, such as the He-Li one. But in this case one is facing another problem, i.e., the contamination of yields by the pre-equilibrium emission prior to the breakup. This contribution is most important for lighter fragments and can be evaluated only on the basis of dynamical simulations.

To apply SMM for analyzing experimental data one needs to know the characteristics (masses, charges, excitation energies) of thermalized emitting sources. A clear identification of such sources is made only in a few cases. One example is given in Ref. [14] where the emitting source with mass 315, charge 126, and a thermal excitation energy of about 5 MeV/nucleon was found for central Au+Au collisions at 35*A* MeV. The SMM calculations reproduce nicely the fragment charge distribution for this reaction yielding the emission temperature of about 6 MeV [14]. By inspecting Fig. 2 one can see that there is no contradiction between the value $T(^{6,7}\mathrm{Li}/^{3,4}\mathrm{He})\approx 4.6$ MeV measured for this reaction [9] and the SMM prediction of $T_{micr}\approx$ 6 MeV. Also in accordance with experiment is that the Be-Li temperature is much higher than other isotopic temperatures. On the other hand, two other isotopic temperatures presented in Fig. 2, $T(^{2,3}\mathrm{H}/^{3,4}\mathrm{He})$and $T(^{7,8}\mathrm{Li}/^{3,4}\mathrm{He})$, are predicted too high and in inverse order compared to $T(^{6,7}\mathrm{Li}/^{3,4}\mathrm{He})$ [9]. Our analysis shows that the yields of neutron-rich isotopes, such as ^{3}H and ^{8}Li, are quite sensitive to the N/Z ratio in the decaying thermalized source. The results of Fig. 2 correspond to the

^{197}Au nucleus with $N/Z \approx 1.5$. The correct ordering of the isotopic temperatures can be achieved by adjusting the N/Z ratio in the source.

Finally we present our analysis of the ALADIN data [2,16] for peripheral Au+Au collisions at 0.6A and 1A GeV (see also [5]). In these experiments only fragments from the projectile spectators were detected. Therefore, here we are dealing with a wide ensemble of emitting sources produced at different impact parameters. As known [17], the masses and excitation energies of these sources are strongly affected by the preequilibrium emission. Nevertheless, the ensemble of thermalized sources can be reconstructed by backtracing the measured characteristics of produced fragments [13,18].

In the SMM calculations presented in Fig. 3 we have considered two different ensembles of emitting sources obtained in Refs. [2] and [13]. The ''experimental'' ensemble of Ref. [2] has a wider distribution in excitation energy (up to about $\varepsilon^* \approx 14$ MeV/nucleon) than the ''theoretical'' ensemble of Ref. [13] which is limited at $\varepsilon^* \approx 8$ MeV/nucleon. As seen from Fig. 3 the observed He-Li temperatures are better reproduced by the experimental ensemble. But this ensemble is certainly contaminated by the early emitted H and He fragments which were not separated in the data analysis. Obviously their admixture is larger at higher excitation energies. On the contrary, in Ref. [13] the sources were reconstructed by using the characteristics of fragments with $Z \geqslant 3$ which are less affected by the pre-equilibrium emission. Therefore, we expect that after separating early emitted H and He fragments experimental points will shift closer to the prediction of the theoretical ensemble.

For both ensembles we get a more steep increase of the isotopic temperature with excitation energy than the experimental data show (Fig. 3, top). Also within the present version of SMM we cannot reproduce the low temperatures extracted from the relative level population in light fragments such as ^{5}Li. Our preliminary calculations show that the agreement with the experiment can be improved by reducing excitation energies of primary fragments and thus suppressing their secondary decay contribution. This and other modifications of the model are under investigation now.

In conclusion, on the basis of SMM we have demonstrated that the secondary deexcitation processes and irregularities in particle-stable excited states of fragments may cause significant deviations of isotopic temperatures from the thermodynamical temperature of the decaying system. Our analysis shows that the ALADIN data are consistent with the anomaly in the nuclear caloric curve. For future studies of the nuclear caloric curve it is very important to separate the contribution of light clusters emitted at early nonequilibrium stages of the reaction. Therefore, the determination of the temperature and excitation energy should be accompanied by a thorough kinematical analysis of emitting sources and fragment spectra.

We thank D.H.E. Gross, W. Friedman, W. Lynch, J. Pochodzalla, U. Schröder, W. Trautmann, and B. Tsang for useful discussions. A.S. Botvina thanks Istituto Nazionale di Fisica Nucleare (Italy) and the Niels Bohr Institute for hospitality and support. I.N. Mishustin thanks the Carlsberg Foundation (Denmark) for financial support. This work was supported in part by the EU-INTAS Grant No. 94-3405.

[1] J. P. Bondorf, R. Donangelo, I. N. Mishustin, and H. Schulz, Nucl. Phys. **A444**, 460 (1985).
[2] J. Pochodzalla *et al.*, Phys. Rev. Lett. **75**, 1040 (1995).
[3] M. B. Tsang, W. G. Lynch, H. Xi, and W. A. Friedman, Report No. MSUCL-1035, 1996.
[4] Y.-G. Ma, Phys. Lett. B **390**, 41 (1997).
[5] R. Wada *et al.*, Phys. Rev. C **55**, 227 (1997).
[6] H. Xi *et al.*, Z. Phys. A **359**, 397 (1997).
[7] S. Albergo *et al.*, Nuovo Cimento A **89**, 1 (1985).
[8] A. Kolomiets *et al.*, Phys. Rev. C **54**, 472 (1996).
[9] M. J. Huang *et al.*, Phys. Rev. Lett. **78**, 1648 (1997).
[10] F. Gulminelli and D. Durand, Nucl. Phys. **A615**, 117 (1997).
[11] D. H. E. Gross, Rep. Prog. Phys. **53**, 605 (1990).
[12] J. P. Bondorf, A. S. Botvina, A. S. Iljinov, I. N. Mishustin, and K. Sneppen, Phys. Rep. **257**, 133 (1995).
[13] A. S. Botvnia *et al.*, Nucl. Phys. **A584**, 737 (1995).
[14] M. D'Agostino *et al.*, Phys. Lett. B **371**, 175 (1996).
[15] A. S. Botvnia, I. N. Mishustin, M. Blann, M. G. Mustafa, G. Peilert, H. Stöcker, and W. Greiner, Z. Phys. A **345**, 297 (1993).
[16] G. Imme *et al.*, GSI Report No. 96-30, Darmstadt, 1996.
[17] A. S. Botvina and I. N. Mishustin, Phys. Lett. B **294**, 23 (1992).
[18] P. Desesquelles, J. P. Bondorf, I. N. Mishustin, and A. S. Botvina, Nucl. Phys. **A604**, 183 (1996).